

# The secondary excited induction generator in random wave input system

Moon-Hwan Kim, Member, KIMICS

**Abstract**—The employment of the induction generator is preferable in the natural energy utilization by the minimum maintenance and the mechanical robustness. Another merit is also expected when it is connected to the power network system, because constant-voltage and constant frequency (CVCF) power generation is easily realized in spite of the variation of the rotor speed. However the induction generator needs much amount of the reactive power that reduces power factor in the primary side. The improvement of power factor in the primary side requires large VAR compensator, this point is solved, the merit of the induction machine as a main generator will become more established. This paper proposes a novel approach where the secondary is controlled by a PWM inverter not only to get CVCF power but also to improve the primary power factor. Basically the inverter is controlled so that the field current is supplied from the secondary side in this approach. The required capacity of the inverter is small, because only the slip power is controlled in the secondary side. In the experimental system where the sea wave torque simulator is used, the power factor is well improved by the microcomputer controlled PWM inverter.

**Index Terms**—Random wave input generation system, CVCF output, wound type induction generator, sea wave

## I. INTRODUCTION

The utilization of the natural energy, such as the wave or wind energy utilization, has been a perpetual wish of the human for a long time. The present days, the necessity of the development of the natural energy become more increased due to the climbing of the crude oil prices and the environmental problems by the rapid progress of the industry. However, since this

natural energy varies randomly, it is difficult to use it effectively. This is because that the output power from the natural energy source always fluctuates statistically and consequently stabilizable controller is indispensable. Recently, the induction generator system tends to be employed as one method to get the CVCF output power from the natural power input generation system.

By directly connecting to the power network, CVCF generation is easily realized without any external power conversion. However, the power factor is reduced as the exciting current is supplied from the primary side. A VAR compensator connected to the primary side will improve the power factor, however it will require a large KVA capacity. On the contrary more active control in the secondary side is possible. In the proposed approach, a novel control of the PWM inverter connected to the secondary brings two following merits. The first merit is the improvement of the power factor. As the natural energy fluctuates statistically, the reactive power will also vary statistically without any control. By supplying the controlled reactive power from the secondary, it is possible to maintain the power factor almost 1.0. The other merit is pointed out since the power factor controller also plays as a CVCF controller, that is convenient when the natural energy generation system is applied to the independent small power system.

The small sized experimental simulator of the random wave power is set up in the laboratory for confirming above features. As an example of the random power generation system, the sea wave generation system is experimentally simulated. The torque simulator synthesizes the input torque of the air turbine for the input wave power based on the statistic method. In this system, the value of the secondary voltage of the induction generator is determined by the PWM inverter to reduce the reactive power in the primary side. This is calculated by the information of the rotor speed, the rotor position and the slip frequency etc. in the microcomputer system. The microcomputer system also commands the secondary frequency. From the experimental results, this system shows the effectiveness to reduce the reactive power in the random wave generation system.

---

Manuscript received May 19, 2009 ; Revised June 1, 2009. Moon-Hwan Kim is with the Department of Automotive Engineering, Silla University, Busan, 617-736, Korea (Tel: +82-51-999-5701, Fax: +82-51-999-5652, Email: mhkim@silla.ac.kr)

## II. SECONDARY EXCITED INDUCTION GENERATOR SYSTEM

The equivalent circuit of secondary excited induction generator is shown in Fig. 1. Here,  $V_1$ ,  $V_2$ ,  $I_1$ , and  $I_2$  are the phase voltages and the line currents of the primary and secondary side of the induction machine and  $r_1$ ,  $r_2/s$ ,  $x_1$  and  $x_2$  are resistances and reactances of the stator and the rotor.  $E$ ,  $I_m$ ,  $x_m$  and  $s$  are the induced voltage, the magnetizing current, the magnetizing reactance and the slip, respectively. In this equivalent circuit, the core loss of the machine is ignored.

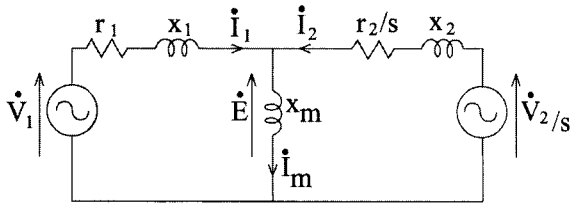


Fig. 1 Equivalent circuit of secondary excited induction generator

From Fig. 1, the relation between the voltage and the current of the primary side can be obtained as shown in eq. (1).

$$\dot{V}_1 = (A + jB)\dot{I}_1 + (C + jD)\dot{V}_2 \quad (1)$$

where,

$$A = \frac{r_1(r_2/s)^2 + r_1(x_2 + x_m)^2 + x_m^2(r_2/s)}{(x_2 + x_m)^2 + (r_2/s)^2}$$

$$B = \frac{x_1(r_2/s)^2 + x_1(x_2 + x_m)^2 + x_m(r_2/s)^2 + x_2x_m(x_2 + x_m)}{(x_2 + x_m)^2 + (r_2/s)^2}$$

$$C = \frac{x_m(x_2 + x_m)/s}{(x_2 + x_m)^2 + (r_2/s)^2}$$

$$D = \frac{x_mr_2/(s)^2}{(x_2 + x_m)^2 + (r_2/s)^2}$$

From the eq. (1), if  $V_1$ , which is the voltage of the connected power system, is constant, the amplitude and phase angle of  $I_1$  can be regulated by the control of  $V_2$ . This means that it can improve the power factor of the primary. The phasor diagram of the induction machine is shown in Fig. 2, where (a) is the case of motor mode, and (b) is the case of generator when the secondary voltage is controlled.

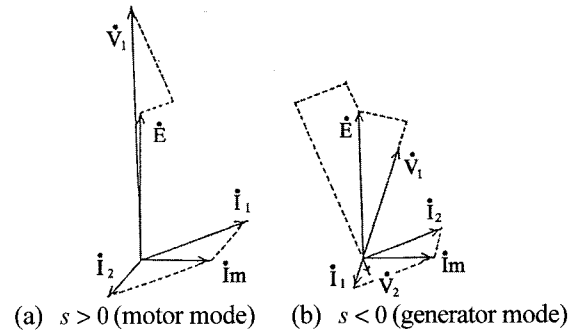


Fig. 2 Phasor diagram of induction machine

## III. CONTROL OF THE REACTIVE POWER

In this paper, the reactive power of the primary is controlled as follows. The one is that the reactive power component of the primary is kept zero. And the other is that the active power component is also kept as same as the value when the secondary side is not controlled.

The eq. (1) is transformed into next eq. (2).

$$\dot{I}_1 = (E + jF)\dot{V}_1 + (G + jH)\dot{V}_2 \quad (2)$$

From this eq. (2), the reactive component of the current  $I_1$  is eliminated by the control of  $V_2$  as shown in eq. (3). The result is also shown in eq. (4).

$$\dot{V}_2 = \frac{(BC - AD) - j(BD + AC)}{(C^2 + D^2)(A^2 + B^2)} B \dot{V}_1 \quad (3)$$

$$\dot{I}_1 = E \cdot \dot{V}_1 \quad (4)$$

By solving eq. (3), the concrete value of  $V_2$  for the control to keep the power factor of the primary unity is acquired. These values are stored in the microcomputer for table-look-up method. Fig. 3 shows one example, where these equations are applied to the tested induction machine of the laboratory.

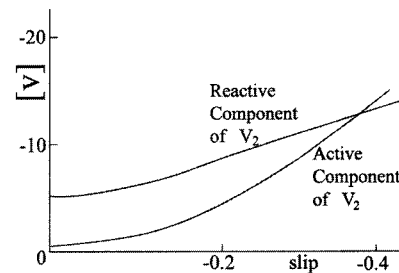


Fig.3 Secondary excitation voltage  $V_2$  ( $V_1=70[V]$ )

In the figure, the curves of active and reactive component of the secondary voltage  $V_2$  vs. slip are calculated according to eq. (3). In this case, the primary voltage  $V_1$  is 70[V]. The reactive power of the primary side, where the secondary is not controlled, and the required reactive power of the secondary to control the power factor of the primary is compared as shown in Fig. 4. When the secondary voltage is controlled, the reactive power of the primary is zero.

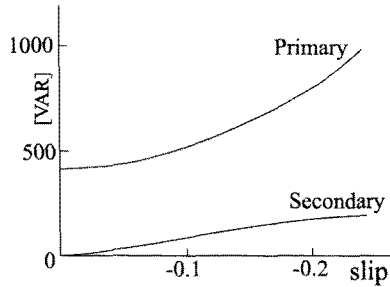


Fig. 4 Reactive power of primary and secondary

This figure shows that the control of the secondary is superior to the control of the primary as to saving KVA capacity of the power converter from the view point of the power factor improvement.

#### IV. APPLICATION TO THE RANDOM WAVE INPUT GENERATION SYSTEM

For applying of the above strategy to the random wave input generation system, it is necessary to overview the total power conversion stage and to clarify the power flow of the random wave input generation system, because the statistic approach is applicable. Here, the sea wave input generation system which is done by JAMSTEC at the sea is analyzed. By the reported method<sup>1)</sup>, the power flow of the system and the torque characteristics are clarified by the data of the real sized experiments. This torque characteristic in frequency domain is difficult to be measures in the real sized experiment. However, this torque characteristic is important to design the basic control strategy of the random wave input generation system, because the torque simulator which reproduces the torque characteristic signal is indispensable in the laboratory level. Fig. 5 shows the simplified power flow diagram of the generation system of the sea wave. Fig. 6 shows the measured and calculated power spectrum density of the input sea wave magnitude (a) and mechanical input torque (b) of the generator.

From Fig. 6, it is pointed out that the major frequency of the variation of the sea wave and the

input torque of the turbine is very low.

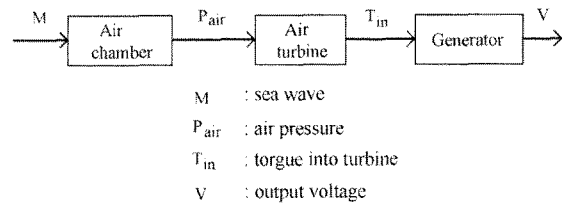


Fig. 5 Simplified power flow diagram of sea wave generation system

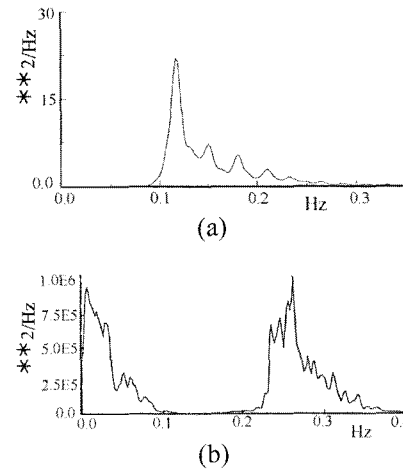


Fig. 6 Power spectrum of sea wave (a) and input torque (b)

Therefore, notwithstanding the above equations (1-4) are the representations for the steady state of the secondary excited induction generator, it is considered reasonable to apply them to the quasi-transient state of the secondary excited induction generation system adopted in the sea wave generation system. The quasi-transient state of the secondary induction generator is simulated by the main-frame computer based on both the statistic approach and the following two axis theory. The exact two-axis theory applied to the six pole machine used in the simulation is shown in the next equations, in which the  $\alpha, \beta$ -axis rotating synchronously with the main magnetic field.

$$\begin{bmatrix} v_{1\alpha} \\ v_{1\beta} \\ v_{2\alpha} \\ v_{2\beta} \end{bmatrix} = \begin{bmatrix} r_1 + L_{\sigma}p & -L_{\sigma}\omega_0 & (M/L_2)p & -(M/L_2)\omega_0 \\ L_{\sigma}\omega_0 & r_1 + L_{\sigma}p & (M/L_2)\omega_0 & (M/L_2)p \\ -(M/L_2)r_2 & 0 & (r_2/L_2) + p & -\omega_0 + 3\omega_m \\ 0 & -(M/L_2)r_2 & \omega_0 - 3\omega_m & (r_2/L_2) + p \end{bmatrix} \begin{bmatrix} i_{1\alpha} \\ i_{1\beta} \\ i_{2\alpha} \\ i_{2\beta} \end{bmatrix} \quad (5)$$

$$i_{2\alpha} = \frac{\lambda_{2\beta} - Mi_{1\beta}}{L_2} \quad (6)$$

$$i_{2\beta} = \frac{\lambda_{2\alpha} - Mi_{1\alpha}}{L_2} \quad (7)$$

$$T = (3/2)(6/2)(\lambda_{2\beta}i_{2\alpha} - \lambda_{2\alpha}i_{2\beta}) \quad (8)$$

where,

$$L_1 = l_1 + M, \quad L_2 = l_2 + M, \quad L_\sigma = \frac{L_1 L_2 - M^2}{L_2}$$

In these equations, the subscription 1 and 2 indicate the primary and second side. And  $\omega_0, \omega_m, L_1, L_2, M, p, \lambda$  are supply frequency, rotor frequency, self inductance of the primary and secondary, mutual inductance, differential operator and flux level, respectively. In the eq. (5), the  $\alpha$  axis synchronously coincides with the voltage vector of the primary, so  $v_{1\alpha}$  is constant and  $v_{1\beta}$  is zero, because the primary is connected to the infinite bus. Therefore, the current  $i_{1\alpha}$  is the active component and the current  $i_{1\beta}$  is the reactive one. In the numerical

calculation, this  $i_{1\beta}$  is controlled to be kept zero by the value of  $V_2$ , which is controlled by eq. (3).

Tested machine is a 2.2kw, 200v, 3phase, 6pole wound-rotor induction generator. The results of the numerical simulation are shown in Fig. 7.  $P_2$  is the waveform of the air pressure of the air chamber.  $N$  is the rotational speed of the generator. Fig. 7-(a) shows the case where the reactive component  $i_{1\beta}$ , is not compensated by  $V_2$ . In Fig. 7-(b), by controlling the secondary voltage  $V_2$ , the reactive current  $i_{1\beta}$ , becomes zero, and the active component  $i_{1\alpha}$ , is the same as shown in Fig. 7-(a).

These results point out that the reactive power of the primary is well reduced by the proposed method where the secondary voltage is controlled by eq. (3).

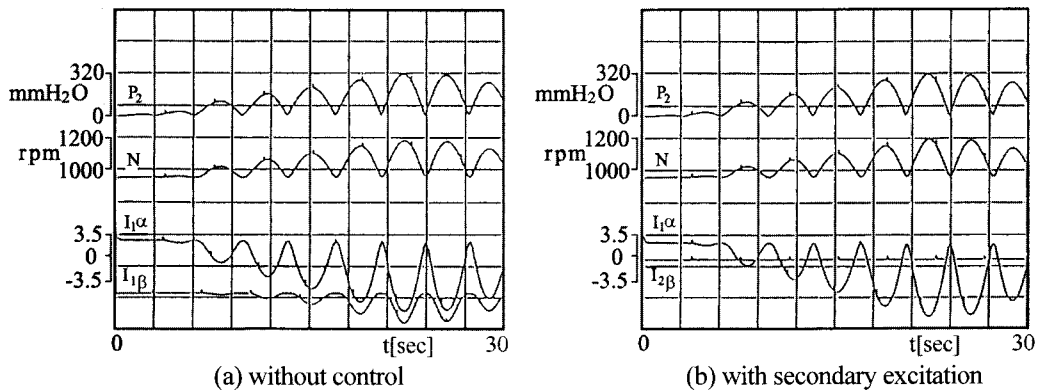


Fig. 7 Results of numerical simulation

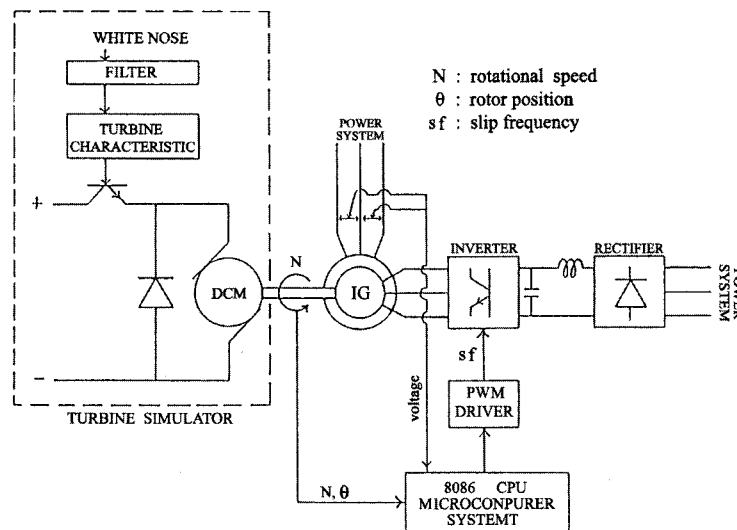


Fig. 8 Schematic diagram of experimental system

### V. EXPERIMENTAL SYSTEM

Above numerical results should be tested by the experiments. In the Fig. 8, the experimental system is shown. The dc motor simulates the torque characteristics of the Fig. 6-(b).

The input torque signal is made from the white noise of the noise generator. In this system, the 8086 microcomputer system is applied as a controller of the PWM inverter. At first, the control of the secondary voltage is carried out in the fixed Cartesian coordinates then transformed into the voltage on the rotor coordinates. For the control, the information of the phase angle and the amplitude of the primary voltage, the calculated slip and so on, decide the phase

angle and amplitude of the secondary voltage in the fixed reference-frame according to the eq. (3). Then this calculated value of the secondary voltage  $V_2$  is transformed into the secondary side. The rotor position is measured by the absolute type rotary encoder. And the rotor winding is supplied by the PWM inverter. These calculations or the decisions of the data are performed by table look-up method for speeding up of the control. The table is constructed by solving the above eq. (3).

And the sampling period to fetch the rotational speed and position and primary voltage is 2msec. It is enough small in comparison with the time period of the sea wave.

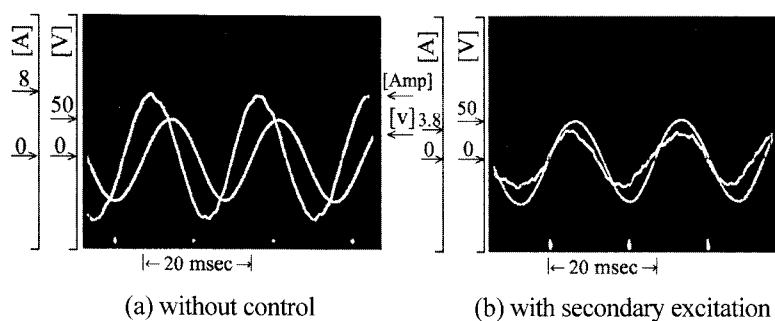


Fig. 9 Voltage and current waveform of the primary

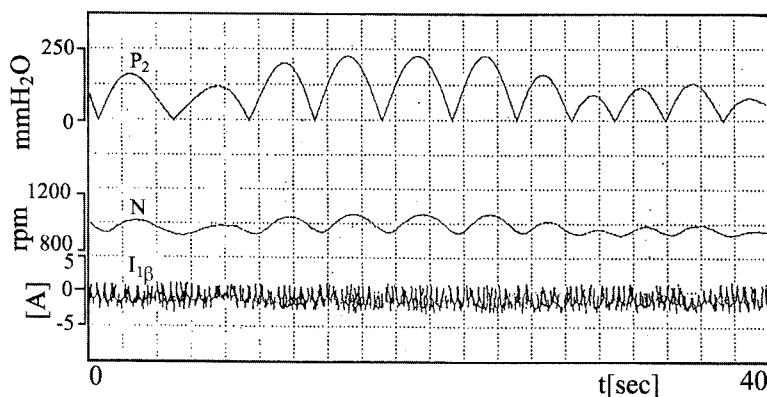


Fig. 10 One example of time response in random wave input generation system based on the proposed control

### VI. EXPERIMENTAL RESULTS

Fig. 9 is the waveform of the primary voltage and current which are improved by control of the PWM inverter. In this figure, the primary voltage is phase voltage and the waveform of the line current is measured by current sensor and reformed by the

computer. The difference of phase becomes more smaller between the voltage and current. Finally, Fig. 10 shows the time response of the system, when the secondary excited generator is driven by the simulated input torque of the sea wave generation system. The upper two waveforms show the variation of the air pressure in the air chamber and the rotational speed of

the air turbine. The lower one shows that  $i_{1\beta}$ , the reactive component of primary current, which is measured by coordinates transformation, is reduced to almost zero. The harmonic components which are observed in the waveform of the current  $i_{1\beta}$  are considered as the induced noise on the measurement devices, such as the switching noise of the PWM inverter and the mechanical vibration of the machine and so on.

These waveforms point out the validity of this power factor improvement method in the random wave input generation system.

## VII. CONCLUSION

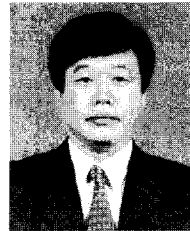
The followings are the results from the analysis, simulations and experiments of this paper.

1. The effectiveness of this method to reduce the reactive power in the random wave input generation system are confirmed by the laboratory experiments by keeping the power factor closely unity in spite of the variation of the rotor speed.

2. The proposed approach requires less KVA capacity of the inverter to control the power factor.

## REFERENCES

- [1] Yokomizo, "Analysis of sea wave generation system of 'Kaimei' type", *Jamstec Experimental report* No.10, pp.97-127, 2. 1983
- [2] Hotta, "The generation performances of sea wave generation system 'Kaimei'", *JSCE symposium*, Tokyo, 6. 1987
- [3] Nagata, "Construction of Offshore Floating Wave Power Device 'Mighty Whale'", *IHI Engineering Review* Vol.33, No.1 pp.24-29 1. 2000
- [4] Washio, "Full-scale performance tests on Tandem Wells turbine", *1st Symposium on wave energy utilization in Japan*, pp.191-199, Tokyo, 11. 1984
- [5] Ohgata, "The present and the future of the sea wave generation", *Energy and resources*, No.132, pp.50-54, 3. 2002
- [6] B.S. Hyun et al., "A Study on the Performance of the Ring-type Impulse Turbine for Wave Energy Conversion", The Korea Committee for Ocean Resources and Engineering, *Journal of Ocean Engineering and Technology*, 1225-0767, Vol.20, No.1, pp.20-25,2006
- [7] Jin Ha Kim et al., "A Study on Motion and Wave Drift Force of a BBDB Type OWC Wave Energy Device", The Korea Committee for Ocean Resources and Engineering, *Journal of Ocean Engineering and Technology*,1225-0767, Vol. 20, No. 2, pp.22-28, 2006
- [8] B.S. Hyun, et al., "Analysis of Impulse Turbine for Wave Energy Conversion Using CFD Method", The Korea Committee for Ocean Resources and Engineering, *Journal of Ocean Engineering and Technology*,pp.1225-0767, Vol. 18, No. 5, pp.1-6, 2004
- [9] J.G. Hwang, "A study on Structure Design of Speed increaser Mechanism for Wave-Force Generator", Korean Society of Precision Engineering, *Proceedings of the Korean Society of Precision Engineering Conference*, pp.1266-1269, 2004
- [10] J.H. Gyeong, "Numerical Analysis on Wave Energy Absorption of OWC-type Wave Power Generation", The Korea Committee for Ocean Resources and Engineering, *Journal of Ocean Engineering and Technology*,1225-0767, Vol. 20, No. 4, pp.64-69, 2006



**Moon-Hwan Kim** received the Ph. D degree in Electrical Engineering from the Keio University, Japan in 1988. He has been with the Division of Automotive Electronic Engineering at Silla University, where he is presently an associate professor.

His research interests are system control and energy conversion system.